

## On the nature of PMSE: Electron diffusion in the vicinity of charged particles revisited

Markus Rapp and Franz-Josef Lübken

Optical Soundings and Sounding Rockets, Leibniz Institute of Atmospheric Physics, Kühlungsborn, Germany

Received 19 August 2002; revised 10 October 2002; accepted 14 October 2002; published 7 February 2003.

[1] Triggered by recent experimental evidence showing that some parts of the *Cho et al.* [1992] theory describing electron diffusion in the vicinity of charged aerosol particles cannot be correct, we reconsider the process of electron diffusion under the conditions of the polar summer mesopause region. The key idea is that perturbations in the distribution of charged aerosol particles created for example by neutral air turbulence almost immediately lead to (anticorrelated) perturbations in the electron number density due to simple charge neutrality and zero net current arguments. We obtain analytical solutions of the coupled diffusion equations for electrons, charged aerosol particles, and positive ions subject to the initial condition of anticorrelated perturbations in the charged aerosol and electron distribution. The main signatures of these solutions are in line with available in situ evidence of small-scale plasma structures in the vicinity of polar mesosphere summer echoes (PMSE), i.e., electron perturbations are anticorrelated to both perturbations in the distributions of negatively charged aerosol particles and positive ions. The lifetime of these perturbations is proportional to the square of the aerosol particle radius such that the presence of particles with radii larger than  $\sim 10$  nm allows for the existence of electron number density perturbations up to several hours after the initial creation mechanism has stopped. These results are almost independent of the ratio between the aerosol charge number density and the number density of free electrons. These electron perturbations potentially give rise to a radar reflectivity comparable to values observed with 50 MHz VHF radars. Our model results can readily explain why in situ measurements of neutral air turbulence have repeatedly shown active turbulence only in the upper part of the PMSE layer whereas turbulence was basically absent in the lower part. Furthermore, our model concept qualitatively yields the correct altitude profile of the mean PMSE occurrence frequency based on the measured altitude profile of the turbulence occurrence frequency. **INDEX TERMS:** 0305 Atmospheric Composition and Structure: Aerosols and particles (0345, 4801); 0340 Atmospheric Composition and Structure: Middle atmosphere—composition and chemistry; 2439 Ionosphere: Ionospheric irregularities; 6929 Radio Science: Ionospheric physics (2409); **KEYWORDS:** PMSE, aerosol particles, neutral air turbulence, mesopause region

**Citation:** Rapp, M., and F.-J. Lübken, On the nature of PMSE: Electron diffusion in the vicinity of charged particles revisited, *J. Geophys. Res.*, 108(D8), 8437, doi:10.1029/2002JD002857, 2003.

### 1. Introduction

[2] Polar mesosphere summer echoes (PMSE) are strong coherent radar echoes from the polar summer mesopause region which were first observed in the VHF band in the late 1970s [Czechowsky *et al.*, 1979; Ecklund and Balsley, 1981]. At these wavelengths radar waves are scattered by electron number density irregularities at the Bragg scale (=radar half wavelength) which is 3 m for a 50 MHz radar. Initially, it was assumed that these irregularities were the direct consequence of enhanced mesospheric turbulence during the polar summer months. However, in situ observations of mesospheric turbulence showed that turbulent energy dissipation rates

were too small by a factor of  $\sim 1000$  in order to directly explain the radar observations (see the study of Lübken *et al.* [2002] for an overview about in situ turbulence measurements inside PMSE). The major breakthrough was then achieved through the work of Kelley *et al.* [1987] who proposed that the electrons in the summer polar mesopause region could be high Schmidt number tracers due to the presence of heavy ion clusters. The Schmidt number  $Sc$  is the ratio of the kinematic viscosity of air and the diffusion coefficient of the tracer under consideration and essentially describes the coupling of the tracer to the neutral gas: i.e., for  $Sc = 1$  the tracer and the neutral gas move together whereas for  $Sc > 1$  perturbations in the tracer can extend to smaller spatial scales because of its reduced diffusivity [Batchelor, 1959]. These ideas were then significantly advanced through the work of Cho *et al.* [1992] who applied the multipolar

diffusion model of *Hill* [1978] to the conditions of the D region plasma in the summer polar mesopause region, i.e., to a plasma consisting of electrons, positive ions and negatively charged ice particles of nanometer size. Essentially, this model work yielded the result that the effective diffusivity of electrons is reduced to the diffusivity of the charged heavy aerosol particles if more than approximately 50% of the negative charge is bound on the particles. Due to this reduced diffusivity, the Schmidt number of the electrons would then be significantly larger than 1 such that electron perturbations at the Bragg scale of a VHF radar indeed had the chance to persist and lead to the radar scatter observed. The main support to this idea came from the observations of so-called electron biteouts, i.e., drastic depletions of the electron number density at the altitudes from which the radar signal was received [*Ulwick et al.*, 1988]. These depletions were interpreted as being due to electron capture by aerosol particles which were known to exist in the vicinity of PMSE from the visual sighting of noctilucent clouds [*Reid*, 1990; *Witt*, 1969]. Thus, at the time of *Cho et al.*'s [1992] work, the picture seemed to be complete: active neutral air turbulence (where the term "active" is defined by the existence of an inertial subrange in the energy spectrum of the velocity field) together with a high Schmidt number of the electrons in the presence of charged aerosol particles provided a physically plausible scenario accounting for PMSE and subsequently, this concept was successfully elaborated by several authors [*Klostermeyer*, 1997; *Chaxel*, 1997; *Hill and Mitton*, 1998; *Hill et al.*, 1999; *Gibson-Wilde et al.*, 2000].

[3] However, in situ observations of neutral air turbulence in the vicinity of PMSE showed that active neutral air turbulence is regularly present in the upper part of the PMSE layer only [*Lübken et al.*, 1993, 2002; *Ulwick et al.*, 1993] whereas it is practically absent in the lower part. In addition, it was found that the Doppler spectra of the observed PMSE were often much too narrow in order to be compatible with the presence of active neutral air turbulence [*Cho et al.*, 1993; *Swartz et al.*, 1993] and it was even suggested that turbulence only acts on preexisting structures in the electron gas rather than creating them [*Röttger*, 1994; *Lübken et al.*, 2002].

[4] Ever since these results, there has been a great effort to find a theoretical explanation of the "nonturbulent" PMSE-type like the dust-hole scatter theory [*Havnes et al.*, 1992], the opalescence theory [*Trakhtengerts and Demekhov*, 1995], and an investigation by *Cho et al.* [1996] who invoked the idea that fossil turbulence (where the term "fossil" is defined by the absence of an inertial subrange in the energy spectrum of the velocity field, but the presence of remnants of formerly active turbulence in the power spectrum of the high Schmidt number tracer) could be of some importance. However, this idea was never really further elaborated in subsequent investigations. For a detailed discussion of these various approaches, we refer the reader to the excellent review article by *Cho and Röttger* [1997] and the more recent investigation by *Rapp et al.* [2003].

[5] However, none of the so far proposed theories has yet been supported by sufficient experimental and/or theoretical evidence such that the question about the "nature of PMSE" must still be considered unanswered.

[6] It is the question of the "nature of PMSE" that we intend to address in the current paper, i.e., we consider

which physical process creates the small-scale electron structures giving rise to the observed radar backscatter: In two recent papers, *Rapp et al.* [2003] and *Blix et al.* [2003] presented substantial evidence that some parts of the electron diffusion theory developed by *Cho et al.* [1992] were not consistent with observational data. In particular, these authors showed that PMSE existed at altitudes where no significant electron depletions were observed thus hinting at the fact that PMSE occurred at altitudes where only a minor fraction of the negative charge was bound to aerosol particles. In such a situation, the *Cho et al.* [1992] theory would not predict a reduced electron diffusivity and hence also no large Schmidt number. On the other hand, *Rapp et al.* [2003] summarized a number of supporting experimental facts which indeed favor the reduced electron diffusivity idea depicted by *Cho et al.* [1992] and they proposed that a few but large charged aerosol particles could also have a significant effect on the electron diffusivity and hence allow for the presence of electron irregularities at the Bragg scale once the structures have been created by a yet unidentified process.

[7] Motivated by these results we reconsider in this paper the question of electron diffusivity in the presence of negatively charged aerosol particles. In section 2, we outline the diffusion theory developed by *Hill* [1978] and discuss its most important property, i.e., the existence of two distinct diffusion modes in the electron gas due to the presence of negatively charged aerosol particles and positive ions. In section 3, we then propose a physical mechanism that has the potential to explain PMSE both in the presence and absence of neutral air turbulence. The main idea is that for example neutral air turbulence initially creates small-scale perturbations in the distribution of charged aerosol particles that are mirrored in the electron and positive ion distribution due to simple charge neutrality and zero net current arguments. Once the excitation mechanism (e.g., neutral air turbulence) ceases it is shown that the irregularities in the electron gas can only decay with the time constant of the aerosol particle perturbations which can be on the order of several 10 min to hours. In section 4, we then discuss whether neutral air turbulence can be the sole excitation mechanism creating the long living small-scale perturbations in the aerosol particle distribution, i.e., we discuss the available statistics of turbulence occurrence rates and PMSE occurrence rates and other experimental facts. Finally, in section 5, we summarize our results and suggest a radar experiment that has the potential to verify or falsify our results.

## 2. Anomalous Electron Diffusion in the Polar Summer Mesopause Region

[8] Since several equations of *Hill*'s [1978] multipolar diffusion theory are needed in the course of this paper, e.g., for the justification of the choice of our initial condition, we have decided to sketch the derivation of *Hill*'s [1978] diffusion equations by stating the most important steps and equations relevant for our own development in section 3. Note, however, that it is certainly not our intention to repeat *Hill*'s [1978] original work such that we do not go into too much detail about algebraical manipulations of the equations, etc. For such information,

the reader is referred to the excellent original article by Hill [1978].

### 2.1. The Hill [1978] Theory

[9] Our investigation of electron diffusion described in section 3 of this paper is based on the work of Hill [1978] who treated the case of quasi-neutral diffusion of a multiconstituent plasma. Quasi neutrality prevails when the inhomogeneities under consideration are significantly larger than the electron Debye length. This situation applies to PMSE conditions in the VHF band: in this case the Debye length is  $\sim 1$  cm while irregularities causing PMSE occur on scales of the radar half wavelength, i.e., at scales of  $\sim 3$  m (=radar half wavelength of a 50 MHz radar). It is further assumed that the neutral gas is at rest, that gravitational settling of the plasma constituents is negligible, and that external electric and magnetic fields can be ignored. Then the steady state equation of motion (per unit volume) of the charged species is given by

$$N_j q_j \vec{E} = \nabla p_j + m_j \nu_j \vec{\Gamma}_j \quad (1)$$

where  $N_j$  is the number density,  $q_j = Z_j e$  the charge ( $e =$  elementary charge),  $\vec{E}$  the multipolar electric field,  $p_j$  the partial pressure,  $m_j$  the mass,  $\nu_j$  the collision frequency with the neutral gas, and  $\vec{\Gamma}_j$  the flux of the  $j$ th plasma constituent. The partial pressure  $p_j$  can be expressed as  $p_j = N_j k T$  where  $k$  is Boltzmann's constant and  $T$  is the temperature (which is the same for all the species at the altitudes under consideration).

[10] It is further useful to introduce the diffusion coefficient  $D_j = kT/(m_j \nu_j)$  and the mobility  $\mu_j = q_j/(m_j \nu_j)$ . With these definitions, (1) can be written as

$$N_j \mu_j \vec{E} = D_j \nabla N_j + \vec{\Gamma}_j \quad (2)$$

If (2) is now multiplied with  $q_j$ , summed over all  $j$  and if it is assumed that  $\sum_j q_j \vec{\Gamma}_j = 0$  (zero net current in or out of any unit volume) the multipolar electric field can be expressed as

$$\vec{E} = \frac{\sum_j q_j D_j \nabla N_j}{\sum_j q_j N_j \mu_j} \quad (3)$$

In order to give an estimate of the magnitude of this multipolar electric field we approximate (3) by its contributions due to free electrons which is reasonable because  $D_e \gg D_{j \neq e}$  and  $\mu_e \gg \mu_{j \neq e}$ . If we further use the definitions of  $D_e$  and  $\mu_e$  we obtain:

$$\vec{E} = -\frac{kT}{e} \frac{1}{N_e} \nabla N_e \quad (4)$$

For example, a relative electron density fluctuation of  $\Delta N_e/N_e = 0.1$  [e.g., Blix and Thrane, 1993] and  $\Delta x = 1$  m appropriate for PMSE leads to an electric field of  $\approx 2$  mV/m for a typical temperature of 150 K.

[11] With the aid of (4), (2) is easily solved for the fluxes  $\vec{\Gamma}_j$ :

$$\vec{\Gamma}_{j \neq e} = -D_j \nabla N_j + \frac{q_j}{q_e} \frac{N_j}{N_e} D_j \nabla N_e \quad (5)$$

We now consider a plasma consisting of electrons, one group of positive ions with number density  $N_i$  and one group of

singly negatively charged aerosol particles with number density  $N_A$ . For the time being we neglect positively charged aerosol particles since the experimental evidence for their existence is still scarce whereas almost each rocket sounding of charged particles in the vicinity of PMSE yielded evidence for negatively charged particles [Havnes et al., 1996b, 2001; Mitchell et al., 2001; Croskey et al., 2001; Smiley et al., 2003]. For each of these species, the continuity equation is

$$\frac{\partial N_j}{\partial t} + \nabla \cdot \vec{\Gamma}_j = 0 \quad (6)$$

Note that we neglect production and loss terms like electron-positive ion pair production, dissociative recombination of electrons and positive ions and electron or ion capture by aerosol particles since we assume that the system is in chemical equilibrium where these contributions to the continuity equation cancel.

[12] Quasi neutrality and zero net current requires  $N_e = N_i - |Z_A|N_A$  and  $\vec{\Gamma}_e = \vec{\Gamma}_i - \vec{\Gamma}_A$ . For algebraical convenience we introduce the quantity  $N_{\oplus} = N_i + N_A$ , i.e., the total number density of plasma species different from electrons. Furthermore, we express the charge number density of the aerosol particles in terms of its abundance relative to electrons, i.e., we introduce the parameter

$$\Lambda = |Z_A|N_A/N_e. \quad (7)$$

Now small perturbations of the number densities are considered, i.e.,  $N_e = N_{e0} + n_e$ ,  $N_i = N_{i0} + n_i$ ,  $N_A = N_{A0} + n_A$ , and  $N_{\oplus} = N_{\oplus 0} + n_{\oplus}$ . Here  $N_{e0}$ ,  $N_{i0}$ ,  $N_{A0}$ , and  $N_{\oplus 0} = N_{i0} + N_{A0}$  are the background number densities of the different species and  $n_e$ ,  $n_i$ ,  $n_A$ , and  $n_{\oplus} = n_i + n_A$  the corresponding small disturbances on top of the background concentrations. With these definitions the use of (5) and (6) leads to the two following continuity equations for  $n_e$  and  $n_{\oplus}$  if nonlinear terms are neglected (note further that the perturbation quantities are assumed to be so small compared to the background that they do not change the chemical equilibrium):

$$\frac{\partial n_e}{\partial t} = \frac{D_i - D_A}{2} \nabla^2 n_{\oplus} + \left[ D_i + \frac{D_i + D_A}{2} (1 + 2\Lambda) \right] \nabla^2 n_e \quad (8)$$

$$\frac{\partial n_{\oplus}}{\partial t} = \frac{D_i + D_A}{2} \nabla^2 n_{\oplus} + \left[ D_i + \frac{D_i - D_A}{2} (1 + 2\Lambda) \right] \nabla^2 n_e \quad (9)$$

where  $D_i$  and  $D_A$  are the diffusion coefficients of positive ions and negatively charged aerosols, respectively. Note that  $\Lambda$  is the ratio of the total number densities of charged aerosol particles and electrons (i.e.,  $|Z_A|N_A$  and  $N_e$ ) which is not necessarily the same as the ratio between the fluctuation densities (i.e.,  $|Z_A|n_A$  and  $n_e$ ) as it was formerly assumed by Cho et al. [1992], Chaxel [1997], and Rapp and Lübken [2000] (see Appendix B for a detailed discussion of (7)).  $n_i$  and  $n_A$  can be derived from  $n_{\oplus}$  and  $n_e$  by means of  $n_i = (n_{\oplus} + n_e)/2$  and  $n_A = (n_{\oplus} - n_e)/2$ , respectively.

### 2.2. Diffusion Modes of the System

[13] Before we consider the temporal development of a small-scale disturbance in the electron density we note that the coupled diffusion system given by (8) and (9) possesses

two eigenmodes (characterized by appropriate eigenvalues of the linear equation system) independent of a particular initial value problem. The eigenvalues are given by:

$$D_{1/2}^0 = \frac{1}{2} [D_i + (D_i + D_A)(1 + \Lambda)] \pm \frac{1}{2} \sqrt{D_i^2(\Lambda + 2)^2 + 2D_i D_A(\Lambda - 2)(\Lambda + 1) + D_A^2(\Lambda + 1)^2} \quad (10)$$

The quantities  $D_{1,2}^0$  have a direct physical meaning: they describe the two diffusion modes of the system due to the electric field between electrons and positive ions (described by  $D_1^0$ ), and between electrons and charged aerosol particles (described by  $D_2^0$ ), respectively. In Figure 1, we present values of  $D_1^0$  and  $D_2^0$  as a function of  $\Lambda$  and  $r_A$ . Here,  $D_i$  and  $D_A$  have been calculated as discussed by *Cho et al.* [1992]:

$$D_i = \frac{3kT}{16\mu_{in}n_n\Omega_{in}} \quad (11)$$

$$D_A = 4.14 \cdot 10^{-7} \sqrt{\frac{e^2\gamma\mu_{in}}{2\epsilon_0kTm_n}} \cdot \frac{D_i}{r_A^2} \quad (12)$$

where  $\mu_{in}$  is the reduced mass of a positive ion and a neutral air molecule,  $n_n$  the neutral air number density, and  $\Omega_{in}$  the collision integral as determined from the polarization interaction model.  $\gamma$  is the neutral atom polarizability,  $m_n$  the mass of an air molecule, and  $r_A$  the radius of the aerosol particle. Typical values for  $D_i$  and  $D_A$  are 0.4 and 0.0017 m<sup>2</sup>/s ( $r_A = 10$  nm), respectively, if we assume positive ions of mass 91 amu ( $H^+(H_2O)_5$ ) which is a dominant ion species at 85 km altitude during polar summer conditions [*Kopp et al.*, 1985].

[14] As evident from Figure 1, the two diffusion coefficients show very different signatures:  $D_1^0$  is basically independent of the aerosol particle size but varies strongly with  $\Lambda$ , i.e., for  $\Lambda$  between 0.01 and 10,  $D_1^0$  increases from  $\sim 0.5$  to  $\sim 5$  m<sup>2</sup>/s. Hence, the presence of negatively charged aerosol particles enhances this diffusion mode.

[15] Compared to this,  $D_2^0$  mainly depends on the aerosol radius and varies over several orders of magnitude between  $\sim 0.1$  and  $10^{-5}$  m<sup>2</sup>/s for the same range of radii. For this eigenmode, however, the  $\Lambda$  dependence is much weaker. Note furthermore that  $D_2^0$  equals  $D_A$  in the case of small  $\Lambda$  values (see also (10)).

### 3. A Physical Mechanism for PMSE

[16] In this section, we consider the role of electron diffusion for the existence of small-scale electron structures giving rise to PMSE. We assume for a moment that some mechanism (e.g., neutral air turbulence) has created small-scale fluctuations in the distribution of charged aerosols which extend to scales smaller than the inner scale of turbulence due to the very large Schmidt number of the aerosol particles ( $Sc \approx 6.5r_A^2 = 650$ , if  $r_A = 10$  nm) [*Batchelor*, 1959; *Lübken et al.*, 1998]. The formation of the charged aerosol particle perturbation creates a flux of charged aerosol particles,  $\Gamma_A$ . According to the zero net current requirement,  $\Gamma_A$  must be balanced by electron and positive ion fluxes, i.e.,  $\Gamma_A = \Gamma_i - \Gamma_e$ .

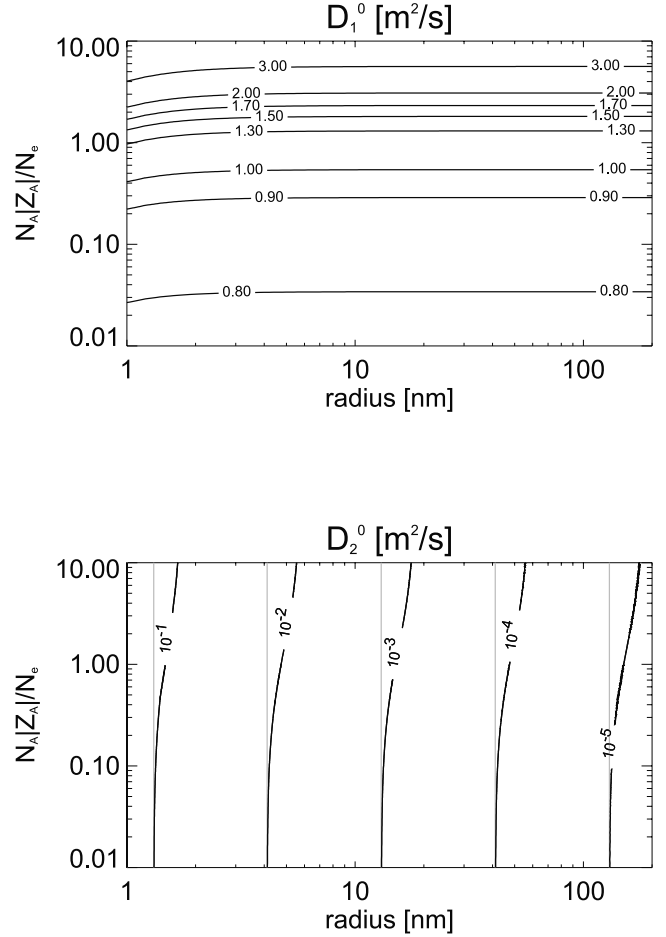


**Figure 1.** Diffusion coefficients  $D_1^0$  (upper panel) and  $D_2^0$  (lower panel, black contours) as a function of  $\Lambda$  and aerosol radius  $r_A$ . The gray lines in the lower panel show corresponding contours of the aerosol diffusion coefficients  $D_A$ .

Combining (2) and (3) and considering that initially there is only a gradient in the distribution of charged aerosol particles we obtain  $\Gamma_e \approx \frac{q_A}{q_e} D_A \nabla N_A$  and  $\Gamma_i \approx \frac{N_{i0}}{N_{e0}} \Gamma_e \approx \frac{m_e}{m_i} \Gamma_e \approx 0$ , where  $m_e$  and  $m_i$  are the masses of an electron and a positive ion, respectively. Thus, fluctuations in the distribution of aerosol particles directly lead to fluctuations in the electron gas whereas the positive ion number density reacts much more slowly than the electrons due to its lower mobility. Later, when  $\Gamma_e$  has caused a substantial perturbation in the electron gas,  $\nabla N_e$  is certainly different from zero such that (5) also yields a positive ion flux which subsequently also creates a perturbation in the positive ions (see our discussion of Figures 2 and 3).

[17] We now want to discuss the case that the creation mechanism (e.g., neutral air turbulence, see section 4) has stopped and leaves aerosol particles, electrons and positive ions to the action of multipolar diffusion. We solve the diffusion equations (8) and (9) for the initial conditions described above, i.e., an initial anticorrelation of negatively charged aerosol particles and electrons. Then we discuss the consequences of our findings for the scattering of radio waves. For a short comment on the differences between our

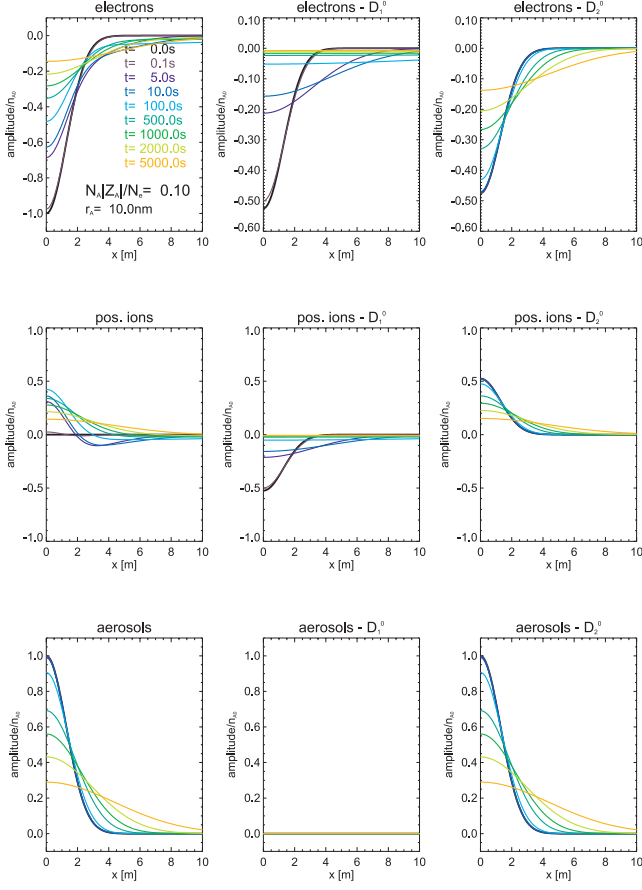


**Figure 2.** Temporal development of electron, positive ion, and charged aerosol particle fluctuations. Panels labeled with  $D_1^0$  and  $D_2^0$ , respectively, show the respective contribution due to the  $D_1^0$  and  $D_2^0$  eigenmode.

results and the results obtained by *Cho et al.* [1992], see Appendix B.

### 3.1. A Special Solution of the Diffusion Equations

[18] As described above we consider initial disturbances in the aerosol charge number density and the electron number density of the form  $n_A(x, t=0) = n_A(0, 0) \cdot \exp(-x^2/2\sigma^2)$  and  $n_e(x, t=0) = -n_A(x, t=0)$ . Hence,  $n_i(x, t=0) = 0$  and  $n_{\oplus}$  satisfies the initial condition  $n_{\oplus}(x, t=0) = n_A(x, t=0)$ . Subject to these initial conditions, we have solved (8) and (9) analytically, yielding the following results:

$$\frac{n_e(x, t)}{n_A(0, 0)} = \frac{D_i - D_1^0}{D_1^0 - D_2^0} \cdot H(D_1^0, x, t) - \frac{D_i - D_2^0}{D_1^0 - D_2^0} \cdot H(D_2^0, x, t) \quad (13)$$

and

$$\begin{aligned} \frac{n_{\oplus}(x, t)}{n_A(0, 0)} = & -\frac{2D_2^0 - (D_i + D_A)}{D_1^0 - D_2^0} \cdot \frac{D_i - D_1^0}{D_i - D_A} \cdot H(D_1^0, x, t) \\ & + \frac{2D_1^0 - (D_i + D_A)}{D_1^0 - D_2^0} \cdot \frac{D_i - D_2^0}{D_i - D_A} \cdot H(D_2^0, x, t) \end{aligned} \quad (14)$$

with

$$H(D, x, t) = \frac{1}{\sqrt{1 + 2Dt/\sigma^2}} \cdot \exp\left(-\frac{x^2/\sigma^2}{2(1 + 2Dt/\sigma^2)}\right) \quad (15)$$

[19] In Figure 2, we show the temporal development of electron, positive ion and charged aerosol particle fluctuations as described by (13) and (14) for  $r_A = 10$  nm. We use a typical value of  $\Lambda = 0.1$  in order to match recently reported experimental values [*Blix et al.*, 2003] and the full width at half maximum of the initial Gaussian has been chosen as 3 m, i.e.,  $\sigma = 3m/2\sqrt{2 \cdot \ln(2)} \approx 1.27$  m. Concentrating first on the solutions for the electron disturbance it appears that the decay process divides into two significantly different parts: while the amplitude of the electron fluctuation decays quickly (i.e., in less than 100 s) from a

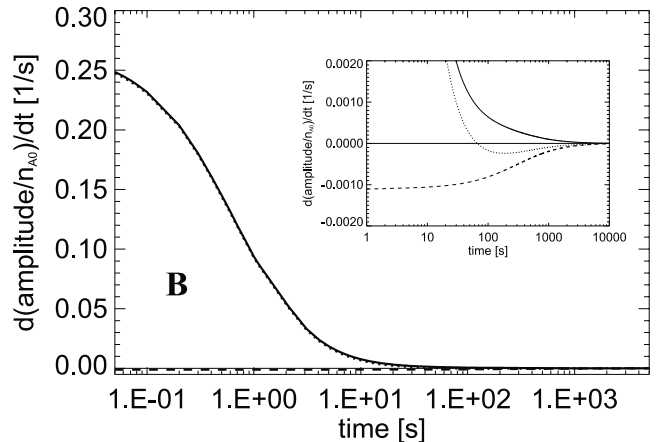
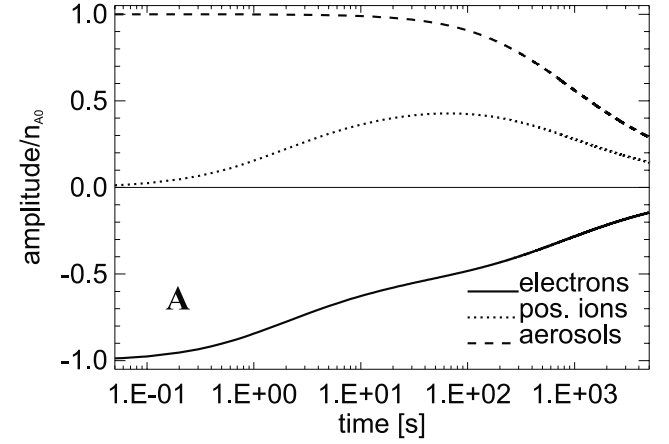


**Figure 3.** Panel A: Temporal evolution of the amplitudes of the electron, positive ion, and charged aerosol particle perturbation for aerosol particles with a radius of 10 nm and  $\Lambda = 0.1$ . Panel B: Rate of amplitude change of the perturbations. The insert shows the rate of change on a smaller amplitude scale revealing that after  $\sim 100$  s the rate of change of the positive ion amplitude is negligible and charged aerosol particles and electrons decay with the same time constant.

value of 1 (in units of  $n_A(0, 0)$ ) to a value of  $\sim 0.5$ , it takes  $\sim 2$  hours to further decay to a value of 0.1. If we look at the contributions to the electron solution due to the  $D_1^0$  and  $D_2^0$  eigenmode, we see that the  $D_1^0$  eigenmode dominates the first period whereas the  $D_2^0$  eigenmode dominates the second period of diffusional decay. The reason for this behavior can be understood if we consider the simultaneous behavior of the positive ions: The electron perturbation creates a polarization electric field between electrons and positive ions giving rise to a positive ion flux of (see (5))  $\Gamma_i \approx -\frac{N_{i0}}{N_{e0}+n_e} D_i \nabla n_e$  and hence (6)  $\frac{\partial n_i}{\partial t} = \frac{N_{i0}}{N_{e0}+n_e} D_i \Delta n_e$ . Considering only  $x = 0$ , this yields  $\frac{\partial n_i}{\partial t} \approx +\frac{D_i}{\sigma^2}$ . In addition,  $\frac{\partial n_e}{\partial t} = \frac{\partial n_i}{\partial t}$  during the first period of diffusion since the initial rate of change of the aerosol particle charge perturbation is very small due to their extremely low mobility. This behavior of the perturbations is depicted in Figure 3 where we show the temporal behavior of the amplitudes of the charged species as well as their rate of change for aerosol particles with a radius of 10 nm and  $\Lambda = 0.1$ . Note that indeed the initial amplitude change rate of positive ions and electrons is given by  $+\frac{D_i}{\sigma^2} \approx \frac{0.4 \text{ m}^2/\text{s}}{(1.27 \text{ m})^2} \approx 0.26 \text{ 1/s}$ .

[20] Figure 3 also shows that for times larger than  $\approx 100$  s the rate of change of the positive ions becomes negligible compared to the changes of charged aerosol particles and electrons. Hence, after the initial period of  $\approx 100$  s electron diffusion is solely determined by the diffusion of the heavy charged aerosol particles. We thus conclude that after a certain time  $t^*$  which is defined by the requirement  $dn_i/dt = 0$  (i.e., the nontrivial solution,  $t^* \neq \infty$ ) we can assume that the further diffusion of electrons is entirely determined by the  $D_2^0$  diffusion mode and hence the diffusional decay of the aerosol particle perturbation. As is shown in the upper panel of Figure 4 this time  $t^*$  strongly depends on the aerosol radius and on  $\Lambda$ , however, for all reasonable combinations of aerosol sizes and  $\Lambda$  values it turns out that  $t^*$  is always only a couple of minutes or even less. After that initial period of relatively fast electron diffusion, the electron perturbation decays with the time constant of the  $D_2^0$  diffusion mode (and hence approximately with the time constant of the aerosol particle perturbation). The amplitude of the electron perturbation has certainly also decayed during the initial period until  $t^*$ . From the lower panel of Figure 4, we see that for typical values of  $\Lambda$  and  $r_A$ , i.e.,  $\Lambda \leq 2$  and  $r_A \leq 50$  nm [Blix *et al.*, 2003; von Cossart *et al.*, 1999] the electron perturbation amplitude is  $\sim 40$ –50% of the initial amplitude of the aerosol particle perturbation. Note that this “residual” electron perturbation amplitude decreases with increasing  $\Lambda$  due to a larger flux of ions into the region of initial perturbation (i.e., from (5), we get  $\Gamma_i \approx -\frac{N_i}{N_e} D_i \nabla n_e = (1 + \Lambda) \cdot D_i \nabla n_e$ ).

### 3.2. Implications for Radio Wave Scattering

[21] In the preceding subsection, we have seen that after a short initial period of a few minutes the diffusion of electrons in the vicinity of charged aerosol particles is dominated by the  $D_2^0$  diffusion mode which is tightly coupled to the very slow diffusion of the aerosol particles. Now, we proceed and consider the radar reflectivity,  $\eta$ , from such an electron perturbation.

[22] We follow Røyrvik and Smith [1984] who determined the radar reflectivity from a one-dimensional perturbation in the electron number density as follows:

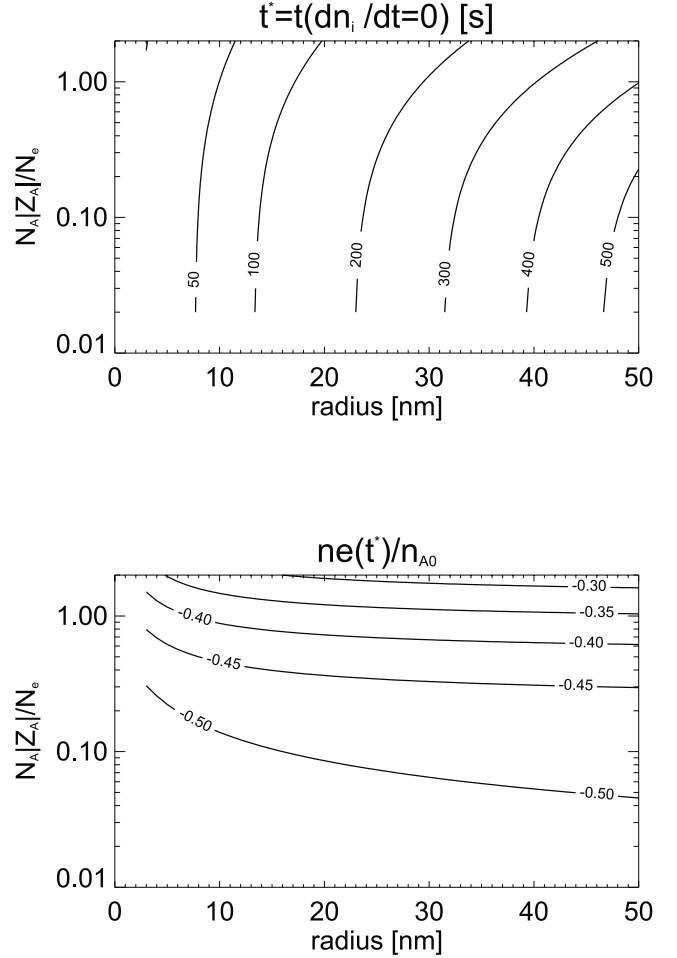


**Figure 4.** Upper panel: Isolines of the time  $t^*$ , which is defined by the requirement that  $dn_i/dt = 0$  as a function of aerosol radius and  $\Lambda$ . Lower panel: Electron density perturbation at the time  $t^*$  for the same range of aerosol radii and  $\Lambda$  values.

$$\eta(k) = -n \frac{\pi}{8} k^2 \frac{f_p^4}{4f^4} \frac{S_{n_e}(k)}{N_e^2} \quad (16)$$

where  $k = \frac{2\pi}{\lambda}$  is the wave number and  $f$  the frequency of the radar,  $f_p = \frac{1}{2\pi} \sqrt{\frac{N_e e^2}{\epsilon_0 m_e}}$  is the plasma frequency depending on the electron number density  $N_e$ , the electron charge  $e$ , the free space permittivity  $\epsilon_0$  and the electron mass  $m_e$ .  $n$  is the exponent of the electron power spectrum at the scales under consideration (i.e., power spectral density  $\propto k^{-n}$ ) and  $S_{n_e}(k)$  is the one dimensional power spectrum of the electron number density perturbation.

[23] We now determine  $S_{n_e}(k)$  assuming that  $t > t^*$  such that the temporal evolution of the electron number density perturbation is entirely determined by the  $D_2^0$  diffusion mode.

[24] As is shown in Appendix A, this leads to the following expression for the radar reflectivity:

$$\eta(k) = -n \frac{k^2}{(8\pi)^3} \frac{e^4}{\epsilon_0^2 m_e^2 f^4} \cdot n_{e0}^2 \cdot \sigma^2 \cdot e^{-k^2 \sigma^2} \cdot \left( \frac{D_i - D_2^0}{D_1^0 - D_2^0} \right)^2 \cdot e^{-2D_2^0 k^2 t} \quad (17)$$

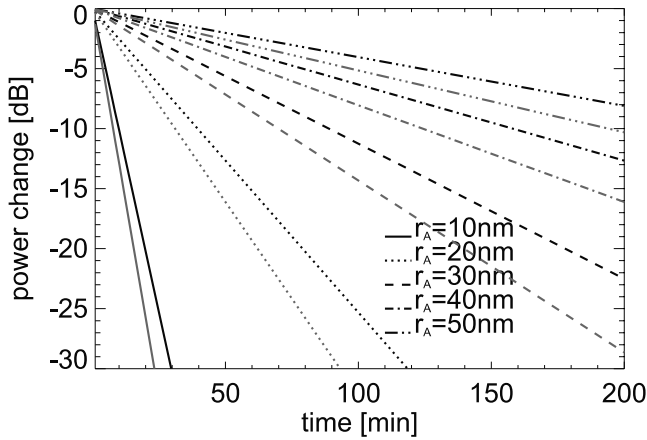


**Figure 5.** Change in signal power due to the diffusional decay of the electron perturbation for aerosol radii between 10 and 50 nm and for two different values of  $\Lambda$ : black lines are for  $\Lambda = 0.1$  and grey lines are for  $\Lambda = 1.0$ .

Using typical values (see next section) of  $n = -3$ ,  $k = 2\pi/6m$ ,  $r_A = 15$  nm,  $\Lambda = 0.1$ ,  $f = 50$  MHz,  $\sigma = 1.27$  m,  $n_{e0} = 250$  cm<sup>-3</sup>, and  $t = 100$  s, we arrive at  $\eta \approx 9 \times 10^{-13}$  m<sup>-1</sup> which is very close to the maximum reflectivity values reported by *Cho and Kelley [1993, Figure 15]*.

[25] How does the radar reflectivity decay if the active mixing process (e.g., neutral air turbulence) stops and the electron perturbations decay according to the factor  $e^{-2D_2^0 k^2 t}$  (see (17))? In Figure 5, we present the change in signal power as a function of time for different aerosol particle radii and two different values of  $\Lambda$ , namely,  $\Lambda = 0.1$  and  $\Lambda = 1.0$ .

[26] As is evident from Figure 5, the decrease of SNR strongly depends on the aerosol radius: for example for  $r_A = 10$  nm the radar signal decreases by 30 dB in approximately 30 min whereas for 20 nm particles the same decrease in SNR already takes between 1.5 and 2 hours. For even larger particles, e.g., 30 nm, the signal decreases by only 15 dB in 2 hours and for the largest particles, e.g.,  $r_A = 50$  nm, the SNR only decreases by 5 dB during as much as 3 hours. In general, the decay time for a decay by  $\Phi$  dB can be calculated from (17) making use of the relation  $10 \cdot \log \left( \frac{\eta(t=\tau_{diff}^{\Phi dB})}{\eta(t=0)} \right) = -\Phi dB$ . Solving this relation for the time  $\tau_{diff}^{\Phi dB}$  yields

$$\tau_{diff}^{\Phi dB} = \frac{\Phi/10 \cdot \ln(10)}{2 \cdot D_2^0 \cdot k^2} \approx \frac{\Phi/10 \cdot \ln(10)}{2 \cdot D_A \cdot k^2} \approx 0.02 \cdot \Phi \cdot \frac{\lambda^2 \cdot r_A^2}{\nu} \quad (18)$$

where we have further used  $D_2^0 \approx D_A$ , the relation  $\frac{\nu}{D_A} \approx 6.5 \cdot r_A^2$  [*Lübken et al., 1998*] and  $k = 2\pi/\lambda$ . Here, the radar wavelength  $\lambda$  is in m, the aerosol radius  $r_A$  in nm and the kinematic viscosity of air,  $\nu$ , is given in m<sup>2</sup>/s. Equation (18) shows that the diffusional decay time is proportional to the square of the radius of the charged particles involved and the square of radar wavelength.

[27] We conclude that PMSE are expected to persist at least a couple of 10 min after active neutral air turbulence has ceased. In the event that larger particles play a significantly role, i.e., at the bottom of the particle layer where the

particles have reached a larger radius due to growth and sedimentation, PMSE can potentially persist for several hours after the active excitation mechanism (=neutral air turbulence) has ceased.

## 4. Discussion

### 4.1. Turbulence as the Prime Excitation Mechanism of PMSE

[28] In the preceding section, we have proposed a physical mechanism for PMSE based on the idea that neutral air turbulence or some other yet unidentified process initially creates the small-scale structures in the aerosol gas which then lead to anticorrelated fluctuations in the electron gas. These fluctuations then decay by ambipolar diffusion where the diffusional lifetime is mainly determined by the diffusional lifetime of the aerosol particle perturbation. Hence, the electron perturbations can survive after the end of active neutral air turbulence for a period between a couple of minutes up to several hours (depending on the aerosol particle radius; see (18)).

[29] We have to note at this point that statements about the lifetime of structures in the electron gas which are on the order of 1 hour or even more must be considered with some care since at these long timescales our assumption of the presence of chemical equilibrium loses its validity. The chemical lifetime is on the order of  $\tau_\alpha = \frac{1}{\alpha \cdot N_e}$  where  $\alpha$  is the dissociative recombination rate for electrons and positive ions, yielding a typical value of  $\tau_\alpha \approx 1000$  s  $\approx 15$  min. However, the lifetime of the perturbation of the charged aerosol particles is on the order of hours (at least if the temperatures are deep enough to avoid premature evaporation of the aerosol particles). Hence even if we imagine that the perturbations of the electron and positive ion number density have been destroyed by recombination, the presence of the charged aerosol particle perturbation will always cause a new perturbation in the other two charged species. Thus, our solutions should at least yield the correct qualitative picture for  $t > \tau_\alpha$ .

[30] Now we take one step further and address the question if neutral air turbulence alone is able to account for all the PMSE observations that are observed or if other mechanisms must also play a role. In order to assess this question we estimate the occurrence frequency of PMSE based on measurements of the occurrence frequency of neutral air turbulence. The PMSE occurrence frequency is estimated as sketched in Figure 6. We start from a given occurrence frequency of neutral air turbulence,  $TOR$ , and assume that a turbulent event lasts  $\tau_{turb} \sim 15$  min. (Actually, typical values of  $\tau_{turb}$  given in the literature range between one buoyancy period ( $\sim 5$  min) and  $\sim 30$  min [*Andreassen et al., 1994; Czechowsky and Rüster, 1997*]. See our discussion of Figure 8 for an investigation of the dependence of the PMSE occurrence frequency on  $\tau_{turb}$ .) We further assume that such a turbulent event leads to an SNR of 15 dB which is a typical mean SNR for PMSE [*Hoffmann et al., 1999*]. Lacking any better information, we further assume that the turbulent events are equally distributed over a given time interval. For example, in Figure 6, we have assumed a typical turbulence occurrence frequency of 25% (see our estimate of the turbulence occurrence rate based on in situ measurements below) such that in a

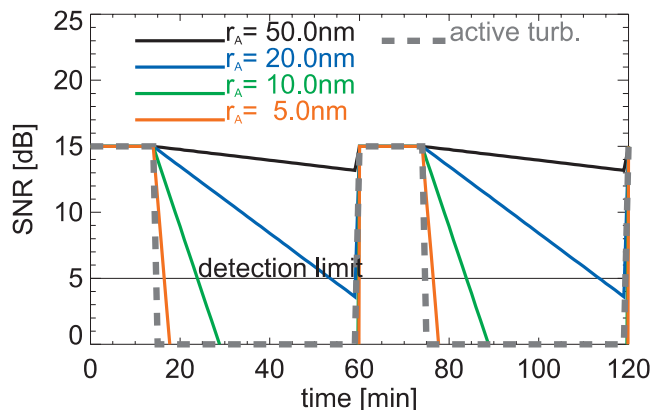


**Figure 6.** Temporal development of the radar SNR after regular pulses of neutral air turbulence (indicated by gray dashed lines) leading to a SNR of 15 dB. The colored lines indicate the SNR decay for different aerosol particle radii assumed. The thin horizontal line at SNR = 5 dB indicates the detection limit assumed.

2-hour interval there are two 15-min events separated each by 45 min.

[31] We calculate the SNR decay after the end of each event according to (17) for a given particle radius. Considering a SNR of 5 dB as a typical detection threshold for PMSE we see that for aerosol particles with  $r_A = 10$  nm (20 nm) the PMSE is expected to last for  $\sim 10$  min (40 min) after active neutral air turbulence has ceased. Adding now these extended time intervals with SNR > 5 dB to the time where turbulence was active and dividing this sum by the total time interval considered, gives an estimate of the occurrence rate of PMSE,  $POR$ , as

$$POR = \begin{cases} TOR \cdot \left(1 + \frac{\tau_{diff}^{-10dB}}{\tau_{turb}}\right); & \text{if } POR < 100 \% \\ 100 \% & ; \text{ else.} \end{cases} \quad (19)$$

In Figure 7, we present results of this estimate for a given altitude distribution of aerosol radii and turbulence occurrence frequencies. In the upper panel of Figure 7, we show the vertical distribution of mean aerosol particle radii that we have chosen according to model results [Rapp *et al.*, 2002, 2003] as well as the corresponding PMSE decay times for a SNR decay by 10 dB (i.e., from 15 to 5 dB). The radius distribution yields small ice particle radii of 2 nm at altitudes around 90 km and  $\sim 60$  nm at 80 km, respectively. In the lower panel of Figure 7, we show the histogram of turbulence occurrence frequencies as a function of altitude which we have determined from the in situ measurements of kinetic energy dissipation rates published by Lübken *et al.* [2002] and the results from two additional rocket flights during a recent rocket campaign conducted at the Andøya Rocket Range in the summer of 2001 (A. Müllemann, private communication). The occurrence frequencies shown are based on the results of 10 sounding rocket flights conducted under PMSE conditions. It turns out that the turbulence occurrence frequency shows a symmetric shape centered at 88 km with a maximum occurrence frequency of 90%, i.e., in 9 out of 10 flights we have found kinetic energy dissipation rates at this altitude. Compared to the

turbulence occurrence frequency we also show the PMSE occurrence frequency obtained in the period from 1 June to 31 July 2000 from measurements with the ALOMAR VHF radar [Latteck *et al.*, 1999] where we have only counted PMSE with SNR > 5 dB. The PMSE occurrence frequency peaks at 85 km with a peak occurrence of 65% and a symmetric distribution between 80 and 90 km. Based on the decay times shown in the upper panel of Figure 7, a Gaussian fit to the turbulence occurrence frequencies, and the assumption that the turbulent events each lasted for 15 min we have estimated the PMSE occurrence frequency based on (19). It turns out that our model indeed gives the correct order of magnitude of the PMSE occurrence

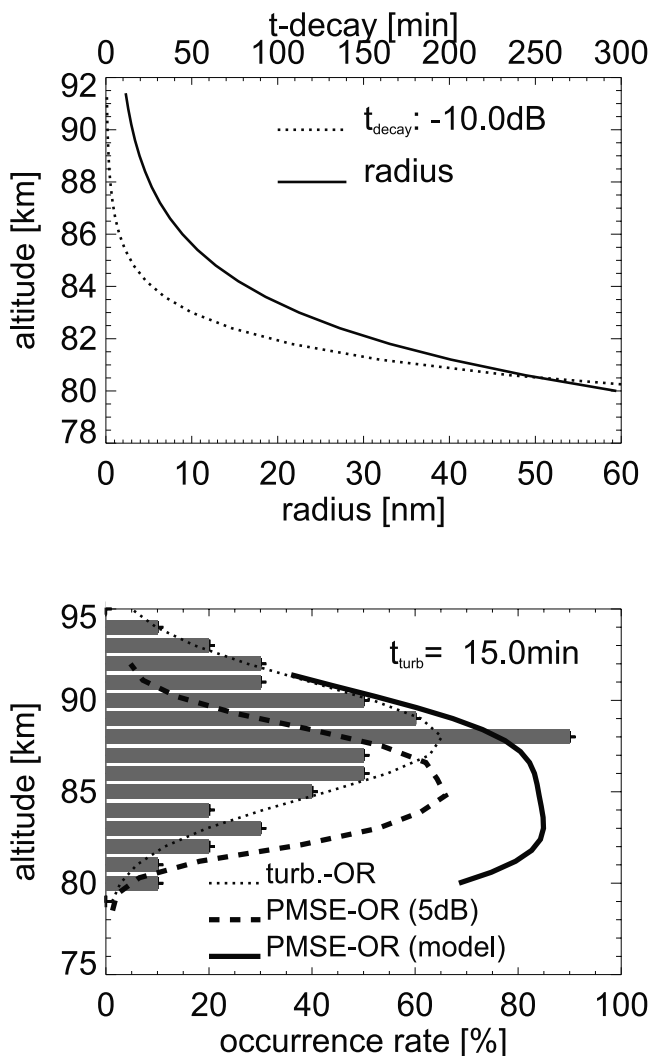


**Figure 7.** Upper panel: assumed aerosol radii (solid lines, lower abscissa) and corresponding decay times for PMSE for a decay by 10 dB (dotted lines, upper abscissa). Lower panel: Histogram of the measured turbulence occurrence rate from a total of 10 rocket soundings [Lübken *et al.*, 2002] together with a Gaussian fit to the data (dotted line). The thick dashed line shows the PMSE occurrence frequency at Andøya in the period from 1 June to 31 July 2000 (only PMSE with SNR > 5 dB were counted) and the thick solid line shows our estimate of the PMSE occurrence frequency.

frequency: We expect PMSE to occur with frequencies between 30 and 90% with peak occurrences just below 85 km. The model overestimates the actual PMSE occurrence frequency because it is assumed that aerosol particles are always there, an assumption that is most likely not correct. Furthermore, we note that all our turbulence measurements have been performed under PMSE conditions what could certainly also bias our estimate of  $TOR$  and hence also  $POR$  to too large values.

[32] Note also that above 89 km the PMSE occurrence frequency is equal to the turbulence occurrence frequency: at these altitudes the aerosol particles are too small to create a major difference between the two quantities since the decay time is short compared to the duration of the turbulent event. However, lower down at 85 km we find that the estimated PMSE occurrence frequency is significantly larger (85%) than the turbulence occurrence frequency (40%). These findings can readily explain why in situ measurements of neutral air turbulence in PMSE have often identified neutral air turbulence in the upper part but not in the lower part of the PMSE layer [Lübken *et al.*, 1993, 2002].

[33] How sensitive are these results to the parameters that we have chosen? In order to address this question we have determined the factor  $\Psi = \frac{POR}{TOR} - 1 = \frac{\tau_{diff}^{-10dB}}{\tau_{turb}}$  both as a function of aerosol radii (and thus  $\tau_{diff}$ ) and the duration of the turbulent event  $\tau_{turb}$  (see Figure 8). The quantity  $\Psi$  is useful to determine how strongly our modeled PMSE occurrence frequencies depend on the assumed turbulence occurrence frequency.  $\Psi \ll 1$  means that basically PMSE can only occur when neutral air turbulence is active,  $\Psi = 1$  already allows for double as much PMSE occurrences as turbulent events, and finally  $\Psi \gg 1$  means that PMSE should be there almost independently of the occurrence of turbulence. Figure 8 shows several interesting features: In general,  $\Psi$  and thus also the possibility to observe PMSE independently from turbulence decreases with an increasing duration of the turbulent event. This is due to the fact that for a given total time with a fixed turbulence occurrence frequency, the increase of the total time with PMSE (total turbulence time + total decay time) is proportional to the number of turbulent events in that period. Clearly, this number decreases with increasing length of the turbulent event.

[34] On the other hand,  $\Psi$  strongly increases with increasing aerosol radius (since it is proportional to  $r_A^2$ ) and it turns out that for radii larger than  $\sim 40$  nm,  $\Psi$  is significantly larger than 1 for all assumed values of  $\tau_{turb}$ . In other words, for aerosol radii which are typical for NLC conditions [von Cossart *et al.*, 1999] the probability to simultaneously observe PMSE is very high, almost independent of the occurrence frequency of turbulence (as long as it is not zero).

[35] However, Figure 8 also shows that already moderately large aerosol particles (e.g.,  $r_A = 15$  nm) lead to  $\Psi$  values between 1 and 2 provided that the duration of the turbulent events is less than 30 min. Finally, even 10 nm particles increase the PMSE occurrence frequency as compared to the turbulence occurrence frequency by at least 20%. The smallest particles, i.e.,  $r_A \approx 5$  nm, will only then efficiently prolong the average time with PMSE as compared to the average time with turbulence if the duration

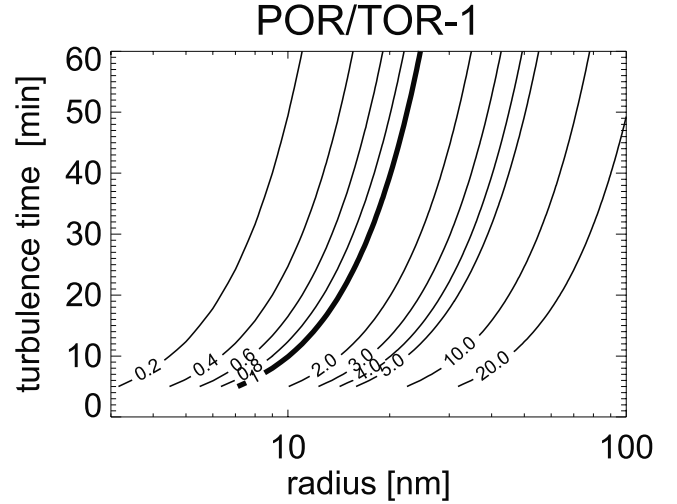


**Figure 8.** Ratio of the PMSE occurrence rate  $POR$  and the turbulence occurrence rate  $TOR$  minus 1 as a function of aerosol radius and the duration of a turbulent event according to (19). The thick black line indicates a value of 1.

of the turbulent event is only one or two buoyancy periods ( $\leq 10$  min). However, here one might also argue that longer turbulence events might also be stronger in intensity such that the corresponding PMSE SNR might be  $\gg 15$  dB (in fact, PMSE observations regularly show SNR values of up to 40 dB). In this case  $\tau_{diff}$  will be significantly longer since the SNR has to decrease by more than 10 dB for the PMSE to disappear (see (18) showing that  $\tau_{diff}$  is directly proportional to the number of dB the PMSE has to decay in order to disappear). Under such conditions, also the smallest particles with  $r_A \approx 5$  nm have the potential to enhance the PMSE occurrence frequency significantly compared to the turbulence occurrence frequency.

[36] Our results imply that at low altitudes (where we expect the largest particles) the PMSE occurrence frequency is expected to be significantly larger than the turbulence occurrence frequency whereas at the upper altitudes where PMSE is usually observed, the PMSE occurrence frequency is identical to the turbulence occurrence frequency. However, since the in situ observations show that there is almost always (strong) turbulence in the upper part of the PMSE altitude range, we conclude that the combination of neutral air turbulence and structures in the electron gas which persist after the end of neutral air turbulence due to a low diffusivity can readily account for all PMSE observations. We note that this statement does not exclude the possibility for alternative mechanisms giving rise to PMSE like a plasma instability [Blix, 1999]. However, we have presented indications that such alternative mechanisms are not necessary in order to explain the statistics of PMSE observations.

#### 4.2. Narrow Doppler Spectra in PMSE

[37] As pointed out in the introduction one of the most intriguing properties of PMSE is the often very narrow Doppler spectrum of the received signal. The Doppler spectrum is expected to be broad in the presence of active neutral air turbulence due to the turbulent velocity fluctua-

tions. According to *Gibson-Wilde et al.* [2000], the velocity variance, which is directly related to the width of the Doppler spectrum, can be expressed in terms of the turbulent energy dissipation rate  $\epsilon$  as

$$\langle w' \rangle = \pm \sqrt{\frac{\epsilon}{5 \cdot 0.4 \omega_B}} \quad (20)$$

where  $\omega_B$  is the mean Brunt frequency over the altitude range where the turbulent event takes place, and the factor 5 is a correction factor to an earlier formula from the study of *Hocking* [1985], which *Gibson-Wilde et al.* [2000] derived from a direct numerical simulation of the VHF radio scatter created by mesospheric turbulence. If we use  $\omega_B = 1.5 \times 10^{-2} \text{ s}^{-1}$  and a rather large value for  $\epsilon$  of  $0.5 \text{ m}^2/\text{s}^3$  for the polar summer mesopause region [*Lübken et al.*, 2002] we see that  $\pm 5.8 \text{ m/s}$  are a typically expected velocity variance due to relatively strong turbulence. Contrary to this, velocity variances measured in PMSE are often less than  $\pm 1 \text{ m/s}$  [*Cho and Kelley*, 1993].

[38] However, in section 3, we have made the point that the electron irregularities are expected to prevail a significant time after the neutral air turbulence has ceased. Under these conditions, however, the velocity variance, which determines the spectral width of the radar echo, is in fact expected to be very small. For example, if we roughly estimate the “minimum” turbulent energy dissipation rate by  $\epsilon_{\min} = \nu \cdot \omega_B^2$  as suggested by *Lübken* [1992] and use  $\nu = 2 \text{ m}^2/\text{s}$  and the same Brunt frequency as before, we get  $\epsilon_{\min} = 0.0005 \text{ m}^2/\text{s}^3$  resulting in  $\langle w' \rangle = 0.1 \text{ m/s}$  which has the correct order of magnitude.

### 4.3. Small-Scale Plasma Fluctuations

[39] Finally, we discuss if the physical mechanism that we have proposed is consistent with experimental results from small-scale plasma and particle measurements inside PMSE.

[40] As pointed out in section 3, the diffusion mechanism predicts that small-scale perturbations in the aerosol particle distribution lead to anticorrelated electron number density perturbations and correlated positive ion number density perturbations. In fact, *Blix and Thrane* [1993] reported anticorrelated small-scale perturbations in the electron and positive ion profiles. Furthermore, *Havnes et al.* [1996a] presented evidence of anticorrelated small-scale perturbations of negatively charged aerosol particles and electrons. More recently, *Mitchell et al.* [2001] have reported similar results. It thus appears that even though all three charged species, i.e., electrons, positive ions, and negatively charged aerosol particles have never been measured in the same volume and with the same altitude resolution, the general picture sketched by our diffusion model of small-scale perturbations in electrons, positive ions and negatively charged aerosol particles is in line with the available in situ evidence.

[41] There is one more interesting point: For a fluid with a high Schmidt number, the *Batchelor* [1959] theory predicts a  $k^{-1}$  power law in the viscous convective subrange, i.e., the subrange between the inertial subrange and the viscous subrange. However, the spectral analysis of small-scale measurements of electron number densities inside PMSE has repeatedly yielded a power law which is much closer to  $k^{-3}$  than to  $k^{-1}$  [e.g., *Ulwick et al.*, 1993].

Note that this is exactly what we expect from the diffusion model discussed in section 3: While during active neutral air turbulence both aerosol particles and electrons are indeed expected to follow a  $k^{-1}$  law, the power spectral densities should fall off considerably steeper after turbulence ceased because the different scales (of length  $L$ ) decay with to a time constant  $\propto \frac{L^2}{D}$  where  $D$  is the effective diffusion coefficient. Hence, small scales decay much more rapidly than larger scales such that after the end of turbulence one expects a power law between  $k^{-1}$  (as expected for the viscous convective subrange) and  $\sim k^{-7}$  (as expected for the viscous subrange [*Heisenberg*, 1948]), i.e., a power law on the order of  $k^{-3}$ .

## 5. Summary and Suggestions for Future Work

[42] We have proposed a physical process which can readily explain the presence of small-scale electron number density perturbations causing PMSE both during the presence of active neutral air turbulence as well as after its decay. The key idea is that neutral air turbulence creates small-scale structures in the distribution of charged aerosol particles, which are mirrored in both electrons and positive ions due to multipolar diffusion. The lifetime of these perturbations is proportional to the square of the aerosol particle radius such that the presence of particles with radii larger than 5–10 nm allows for the existence of electron number density perturbations giving rise to a radar reflectivity comparable to observed values a significant time after the end of neutral air turbulence (e.g., in the case of  $r_A = 20 \text{ nm}$ :  $\tau_{\text{diff}}^{10\text{dB}} = 50 \text{ min}$ ). Most importantly, these model results can readily explain why in situ measurements of turbulence in the vicinity of PMSE have almost always shown no sign of turbulent activity in the lower part of the PMSE layer, since we expect large particles and thus long diffusional lifetimes of electron perturbations below  $\sim 85 \text{ km}$  due to the growth and sedimentation scenario of mesospheric ice particles. Also the fact that turbulence is often found in the upper part of the PMSE is in line with our arguments since above  $\sim 85 \text{ km}$  we expect the ice particles to be rather small and hence the diffusive decay times are short compared to the duration of a turbulent event. At these altitudes, the PMSE occurrence should follow the turbulence occurrence almost one by one.

[43] Furthermore, our model approach explains observations presented by *Röttger* [1994] which led to the conclusion that turbulence acted on preexisting structures in the electron gas. Indeed, our model suggests that these preexisting structures were remnants of a previous turbulent event that persisted in the electron gas due its ambipolar coupling to the perturbations in the aerosol particle distribution with lifetimes on the order of several 10 min up to hours.

[44] In addition, we have also offered an explanation why previous results implying that electron diffusivity should only be reduced if the ratio between the absolute aerosol charge density and the number density of electrons is larger than  $\sim 1$  are most probably flawed due to the assumption of an unrealistic initial condition, i.e., the assumption that initially there should be a positive correlation between charged aerosol particles, electrons, and positive ions (see Appendix B). Contrary to this, the initial condition that we

have assumed as well as the subsequent temporal development of the perturbations in the different plasma species is in line with all published in situ observations of small-scale plasma structures in the polar summer mesopause region.

[45] Finally, the available statistics of the turbulence occurrence frequency combined with our proposed physical process has led to an estimate of the occurrence frequency of PMSE which is close to observational values and thus lends significant support to our idea. We note that the available database of turbulence measurements is scarce (only ten sounding rocket measurements during PMSE) such that further experimental data of the relative time-resolved occurrence of turbulence and PMSE are badly needed. Common volume measurements of PMSE with a VHF radar and the measurement of turbulent parameters with a narrow-beam MF radar have the potential of shedding more light on the question if neutral air turbulence and the “after burning” of the plasma in the presence of charged aerosol particles are the sole reason for the intriguing phenomenon of PMSE. If our approach turns out to be true, spectral width measurements in PMSE (in combination with recent results from direct numerical simulations of mesospheric turbulence) are applicable as a monitor of neutral air turbulence in the polar summer mesopause region.

## Appendix A: Derivation of (17)

[46] For  $t > t^*$ , the electron density perturbation can be approximated as

$$\frac{n_e(x, t)}{n_A(0, 0)} \approx -\frac{D_i - D_2^0}{D_1^0 - D_2^0} \cdot H(D_2^0, x, t) \quad (\text{A1})$$

Hence,  $S_{n_e}(k)$  is given by

$$\begin{aligned} S_{n_e}(k) &\approx \left| \frac{1}{\sqrt{2\pi}} \int_{-\infty}^{+\infty} n_{e0} \cdot \frac{D_i - D_2^0}{D_1^0 - D_2^0} \cdot H(D_2^0, x, t) \cdot e^{-ikx} \cdot dx \right|^2 \\ &\approx n_{e0}^2 \cdot \left( \frac{D_i - D_2^0}{D_1^0 - D_2^0} \right)^2 \cdot |\mathcal{F}(H(D_2^0, x, t))|^2 \end{aligned} \quad (\text{A2})$$

where  $\mathcal{F}(H(D_2^0, x, t))$  is the Fourier transform of  $H(D_2^0, x, t)$  and we have used the initial condition, i.e.,  $|n_A(0, 0)| = |n_e(0, 0)| = n_{e0}$ . With the help of the identity  $\mathcal{F}(e^{-ax^2}) = \frac{\sqrt{2\pi}}{2} \frac{1}{\sqrt{a}} e^{-\frac{k^2}{4a}}$  [e.g., Zeidler, 1996, p. 192] it can be easily shown that

$$\mathcal{F}(H(D_2^0, x, t)) = \sigma \cdot e^{-\frac{k^2 \sigma^2}{2}} \cdot e^{-D_2^0 k^2 t} \quad (\text{A3})$$

and hence

$$S_{n_e}(k) \approx n_{e0}^2 \cdot \left( \frac{D_i - D_2^0}{D_1^0 - D_2^0} \right)^2 \cdot \sigma^2 \cdot e^{-k^2 \sigma^2} \cdot e^{-2D_2^0 k^2 t} \quad (\text{A4})$$

Inserting this result for  $S_{n_e}(k)$  into (16) and making use of the definition of the plasma frequency  $f_p$  then finally yields (17).

## Appendix B: A Side Note on the Cho et al. [1992] Theory

[47] In this appendix, we address the differences of our results to the results formerly obtained by Cho et al. [1992].

In particular, we address why Cho et al. [1992] concluded that electron diffusion should only be reduced for  $\Lambda$  values larger than  $\sim 1$  (whereas we find that it happens for almost all reasonable values of  $\Lambda$ ) and why this diffusivity reduction occurred almost discontinuously.

[48] It turns out that the criticized  $\Lambda \sim 1$  condition of Cho et al. [1992] is due to their particular choice of initial conditions: following the original work by Hill [1978], Cho et al. [1992] (as well as Chaxel [1997] and Rapp and Lübken [2000]) kept the ratios of the electron, charged aerosol and positive ion perturbations equal to their background values, i.e., they assumed that [Cho, 1993, p. 153, line 11ff]:

$$\Lambda = \frac{|Z_A|N_A}{N_e} = \frac{|Z_A|n_A}{n_e} \quad (\text{B1})$$

Thus, they started their calculations with a positive correlation of negatively charged aerosol particles and electrons instead of the anticorrelation that we have assumed.

[49] Hill [1978] had analytically solved (8) and (9) for initially Gaussian disturbances in electrons, charged aerosol particles and positive ions, satisfying (B1). We use these analytical solutions given by Hill [1978, equations (B1a)–(B1e)] in order to demonstrate that the special choice of the initial condition (B1) leads to the features emphasized by Cho et al. [1992]: In Figure 9, we present results of the temporal evolution of the amplitude of an electron disturbance for  $\Lambda$  values of 0.1, 0.5, and 1.5. Similar to the study of Cho et al. [1992], we now measure the time until the electron amplitude finally reaches a given value, we choose  $n_e/n_{e0} = \pm 0.1$ . Figure 9 shows that the parameter  $\Lambda$  determines the relative weight of the  $D_1^0$  and  $D_2^0$  diffusion mode to the complete solution for  $n_e$ : Once  $\Lambda$  is large enough to let the  $D_2^0$  mode make such a significant contribution to the full solution that the perturbation amplitude becomes less than the threshold value (i.e.,  $-0.1$ ) the decay time of the electron perturbation suddenly increases from  $\sim 100$  s (for  $\Lambda = 0.5$ ) to  $\sim 3000$  s for  $\Lambda = 1.5$ .

[50] Note, however, that this discontinuous-like behavior is only due to the initial condition (B1) and that the actual  $\Lambda$  value at which the discontinuity occurs is determined by the threshold that the electron amplitude has to reach (in our case  $\pm 0.1$ ).

[51] We further note that we consider the initial condition (B1) unphysical mainly due to two reasons: first of all  $|Z_A|n_A = \Lambda \cdot n_e$  implies an initial (positive) correlation of electrons and negatively charged aerosols when the diffusion process starts. This conditions seems to be at odds with the fact that Coulomb repulsion will always try to force an anticorrelation between equally charged species. Second, we note that  $|Z_A|n_A = \Lambda \cdot n_e$  implies that  $d|Z_A|N_A/dz = \Lambda \cdot dN_e/dz$  if the fluctuations were assumed to be due to a mixing process in the neutral gas (which was Hill’s [1978] original motivation to use this initial condition; see the last paragraph on page 992 of Hill’s paper) such that  $|Z_A|n_A = d|Z_A|N_A/dz \cdot \Delta z = \Lambda \cdot dN_e/dz \cdot \Delta z$ , where  $\Delta z$  is the vertical displacement of an air parcel during the mixing process. This, however, implies that the gradients  $d|Z_A|N_A/dz$  and  $dN_e/dz$  had the same sign originally, whereas in an electron biteout situation (which is regularly found at PMSE

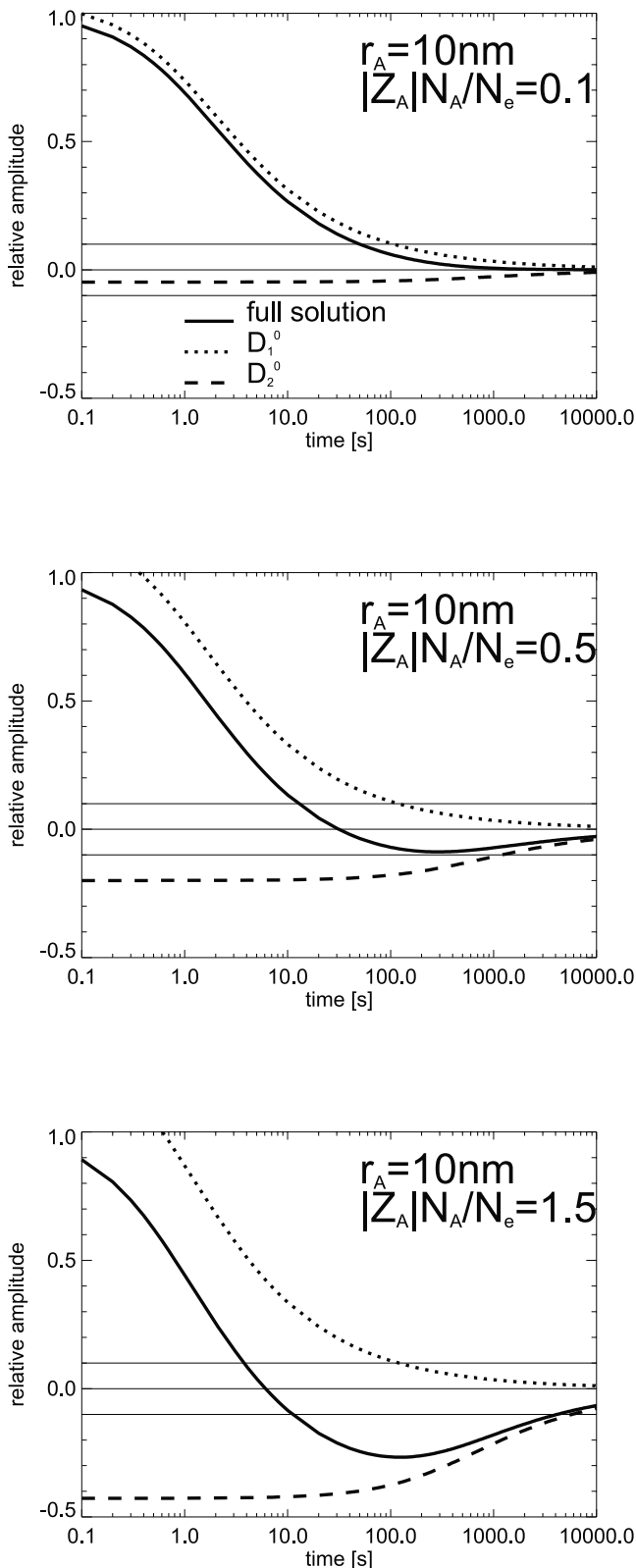


**Figure 9.** Temporal development of the amplitude of an initially Gaussian electron disturbance in the presence of negatively charged aerosol particles with  $r_A = 10$  nm and  $\Lambda$  values of 0.1 (upper panel), 0.5 (middle panel), and 1.5 (lower panel). Dotted and dashed lines show the contribution of the  $D_1^0$  and  $D_2^0$  diffusion mode to the full solution. Horizontal lines mark amplitude values of 0 and  $\pm 0.1$ .

altitudes) one would rather expect  $d|Z_A|N_A/dz = -dN_e/dz$  [e.g., *Klostermeyer*, 1997].

[52] **Acknowledgments.** We acknowledge continued stimulating discussions with J. Gumbel and T. A. Blix. Furthermore, we are indebted to P. Hoffmann for making available the yet unpublished altitude profile of the PMSE occurrence rate shown in Figure 7. The rocket soundings of turbulence were supported by the Bundesministerium für Bildung, Wissenschaft, Forschung und Technologie, Bonn, under grants 01 OE 88027 and 50 OE 98020.

## References

- Andreassen, O., C. Wasberg, D. Fritts, and J. Isler, Gravity wave breaking in two and three dimensions, 1, Model description and comparison of two-dimensional evolutions, *J. Geophys. Res.*, *99*, 8095–8108, 1994.
- Batchelor, G. K., Small-scale variation of convected quantities like temperature in a turbulent fluid, *J. Fluid Mech.*, *5*, 113–133, 1959.
- Blix, T. A., Small scale plasma and charged aerosol variations and their importance for polar mesosphere summer echoes, *Adv. Space Res.*, *24*, 537–546, 1999.
- Blix, T. A., and E. Thrane, Noctilucent clouds and regions with polar mesospheric summer echoes studied by means of rocket-borne electron and ion DC-probes, *Geophys. Res. Lett.*, *20*, 2303–2306, 1993.
- Blix, T. A., M. Rapp, and F.-J. Lübken, Relations between small scale electron number density fluctuations, radar backscatter and charged aerosol particles, *J. Geophys. Res.*, *108*, doi:10.1029/2002JD002430, in press, 2003.
- Chaxel, Y., Radar and modelling studies of polar mesospheric summer echoes, Ph.D. thesis, Univ. Coll., London, 1997.
- Cho, J., W. Swartz, M. Kelley, and C. Miller, CUPRI observations of PMSE during salvo B of NLC-91: Evidence of both partial reflection and turbulent scatter, *Geophys. Res. Lett.*, *20*, 2291–2294, 1993.
- Cho, J. Y., and M. C. Kelley, Polar mesosphere summer radar echoes, *Rev. Geophys.*, *31*, 243–265, 1993.
- Cho, J. Y., C. M. Alcala, M. C. Kelley, and W. E. Swartz, Further effects of charged aerosols on summer mesospheric radar scatter, *J. Atmos. Terr. Phys.*, *58*, 661–672, 1996.
- Cho, J. Y. N., Radar scattering from the summer polar mesosphere: Theory and observations, Ph.D. thesis, Cornell Univ., Ithaca, N. Y., 1993.
- Cho, J. Y. N., and J. Röttger, An updated review of polar mesosphere summer echoes: Observation, theory, and their relationship to noctilucent clouds and subvisible aerosols, *J. Geophys. Res.*, *102*, 2001–2020, 1997.
- Cho, J. Y. N., T. M. Hall, and M. C. Kelley, On the role of charged aerosols in polar mesosphere summer echoes, *J. Geophys. Res.*, *97*, 875–886, 1992.
- Croskey, C., J. Mitchell, M. Friedrich, K. Torkar, U.-P. Hoppe, and R. Goldberg, Electrical structure of pmse and nlc regions during the dropps program, *Geophys. Res. Lett.*, *28*, 1427–1430, 2001.
- Czechowsky, P., and R. Rüster, VHF radar observations of turbulent structures in the polar mesopause region, *Ann. Geophys.*, *15*, 1028–1036, 1997.
- Czechowsky, P., R. Rüster, and G. Schmidt, Variations of mesospheric structures in different seasons, *Geophys. Res. Lett.*, *6*, 459–462, 1979.
- Ecklund, W. L., and B. B. Balsley, Long-term observations of the arctic mesosphere with the MST radar at Poker Flat, Alaska, *J. Geophys. Res.*, *86*, 7775–7780, 1981.
- Gibson-Wilde, D., J. Werne, D. Fritts, and R. Hill, Direct numerical simulation of VHF radar measurements of turbulence in the mesosphere, *Radio Sci.*, *35*, 783–798, 2000.
- Havnes, O., F. Melandsø, C. L. Hoz, T. K. Aslaksen, and T. Hartquist, Charged dust in the Earth's mesopause: Effects on radar backscatter, *Phys. Scr.*, *45*, 535–544, 1992.
- Havnes, O., L. I. Næsheim, T. Hartquist, G. E. Morfill, F. Melandsø, B. Schleicher, J. Trøim, T. Blix, and E. Thrane, Meter-scale variations of the charge carried by mesospheric dust, *Planet. Space Sci.*, *44*, 1191–1194, 1996a.
- Havnes, O., J. Trøim, T. Blix, W. Mortensen, L. I. Næsheim, E. Thrane, and T. Tønnesen, First detection of charged dust particles in the Earth's mesosphere, *J. Geophys. Res.*, *101*, 10,839–10,847, 1996b.
- Havnes, O., A. Brattli, T. Aslaksen, W. Singer, R. Latteck, T. Blix, E. Thrane, and J. Trøim, First common volume observations of layered plasma structures and polar mesospheric summer echoes by rocket and radar, *Geophys. Res. Lett.*, *28*, 1419–1422, 2001.
- Heisenberg, W., Zur statistischen Theorie der Turbulenz, *Z. Phys.*, *124*, 628–657, 1948.
- Hill, R. J., Nonneutral and quasi-neutral diffusion of weakly ionized multi-constituent plasma, *J. Geophys. Res.*, *83*, 989–998, 1978.

- Hill, R. J., and K. A. Mitton, Turbulence-induced ionization fluctuations in the lower ionosphere, *NOAA Tech. Rep. 454-ETL 68*, pp. 1–112, 1998.
- Hill, R. J., D. E. Gibson-Wilde, J. A. Werne, and D. C. Fritts, Turbulence-induced fluctuations in ionization and application to PMSE, *Earth Planet. Space*, *51*, 499–513, 1999.
- Hocking, W. K., Measurement of turbulent energy dissipation rates in the middle atmosphere by radar techniques: A review, *Radio Sci.*, *20*, 1403–1422, 1985.
- Hoffmann, P., W. Singer, and J. Bremer, Mean seasonal and diurnal variation of PMSE and winds from 4 years of radar observations at ALOMAR, *Geophys. Res. Lett.*, *26*, 1525–1528, 1999.
- Kelley, M. C., D. T. Farley, and J. Röttger, The effect of cluster ions on anomalous VHF backscatter from the summer polar mesosphere, *Geophys. Res. Lett.*, *14*, 1031–1034, 1987.
- Klostermeyer, J., A height- and time-dependent model of polar mesosphere summer echoes, *J. Geophys. Res.*, *102*, 6715–6727, 1997.
- Kopp, E., P. Eberhardt, U. Herrmann, and L. Björn, Positive ion composition of the high latitude summer D-region with noctilucent clouds, *J. Geophys. Res.*, *90*, 13,041–13,051, 1985.
- Latteck, R., W. Singer, and H. Bardey, The ALWIN MST radar: Technical design and performance, in *Proceedings of the 14th ESA Symposium on European Rocket and Balloon Programmes and Related Research, Potsdam, Germany, ESA SP*, vol. 437, pp. 179–184, Eur. Space Agency, Noordwijk, Neth., 1999.
- Lübken, F. J., On the extraction of turbulent parameters from atmospheric density fluctuations, *J. Geophys. Res.*, *97*, 20,385–20,395, 1992.
- Lübken, F.-J., G. Lehmacher, T. Blix, U.-P. Hoppe, E. Thrane, J. Cho, and W. Swartz, First in-situ observations of neutral and plasma density fluctuations within a PMSE layer, *Geophys. Res. Lett.*, *20*, 2311–2314, 1993.
- Lübken, F.-J., M. Rapp, T. Blix, and E. Thrane, Microphysical and turbulent measurements of the Schmidt number in the vicinity of polar mesosphere summer echoes, *Geophys. Res. Lett.*, *25*, 893–896, 1998.
- Lübken, F.-J., M. Rapp, and P. Hoffmann, Neutral air turbulence and temperatures in the vicinity of polar mesosphere summer echoes, *J. Geophys. Res.*, *107*, 10.1029/2001JD000915, 2002.
- Mitchell, J., C. Croskey, and R. Goldberg, Evidence for charged aerosol particles and associated meter-scale structure in identified PMSE/NLC regions, *Geophys. Res. Lett.*, *28*, 1423–1426, 2001.
- Rapp, M., and F.-J. Lübken, Electron temperature control of PMSE, *Geophys. Res. Lett.*, *27*, 3285–3288, 2000.
- Rapp, M., F.-J. Lübken, A. Müllemann, G. E. Thomas, and E. J. Jensen, Small scale temperature variations in the vicinity of NLC: Experimental and model results, *J. Geophys. Res.*, *107*(D19), 4392, doi:10.1029/2001JD001241, 2002.
- Rapp, M., F.-J. Lübken, P. Hoffmann, R. Latteck, G. Baumgarten, and T. A. Blix, PMSE dependence on aerosol charge, number density and aerosol size, *J. Geophys. Res.*, *108*, doi:10.1029/2002JD002650, in press, 2003.
- Reid, G. C., Ice particles and electron “bite-outs” at the summer polar mesopause, *J. Geophys. Res.*, *95*, 13,891–13,896, 1990.
- Röttger, J., Polar mesosphere summer echoes: Dynamics and aeronomy of the mesosphere, *Adv. Space Res.*, *14*, 123–137, 1994.
- Røyrvik, O., and L. G. Smith, Comparison of mesospheric VHF radar echoes and rocket probe electron concentration measurements, *J. Geophys. Res.*, *89*, 9014–9022, 1984.
- Smiley, B., S. Robertson, M. Horanyi, T. Blix, M. Rapp, R. Latteck, and J. Gumbel, Measurement of negatively and positively charged particles inside PMSE during MIDAS SOLSTICE 2001, *J. Geophys. Res.*, *108*, doi:10.1029/2002JD002425, in press, 2003.
- Swartz, W., J. Cho, and C. Miller, CUPRI system configuration for NLC-91 and observations of PMSE during Salvo A, *Geophys. Res. Lett.*, *20*, 2287–2290, 1993.
- Trakhtengerts, V. Y., and A. G. Demekhov, Nonequilibrium electron density fluctuations and wave scattering in the mesosphere, *J. Atmos. Terr. Phys.*, *57*, 1153–1164, 1995.
- Ulwick, J. C., K. D. Baker, M. C. Kelley, B. B. Balsley, and W. L. Ecklund, Comparison of simultaneous MST radar and electron density probe measurements during STATE, *J. Geophys. Res.*, *93*, 6989–7000, 1988.
- Ulwick, J. C., M. C. Kelley, C. Alcala, T. Blix, and E. V. Thrane, Evidence for two different structuring and scattering mechanisms and the associated role of aerosols in the polar summer mesosphere, *Geophys. Res. Lett.*, *20*, 2307–2310, 1993.
- von Cossart, G., J. Fiedler, and U. von Zahn, Size distributions of nlc particles as determined from 3-color observations of nlc by ground-based lidar, *Geophys. Res. Lett.*, *26*, 1513–1516, 1999.
- Witt, G., The nature of noctilucent clouds, *Space Res.*, *IX*, 157–169, 1969.
- Zeidler, E., *Teubner-Taschenbuch der Mathematik*, Teubner Verlag, Stuttgart, 1996.

---

F.-J. Lübken and M. Rapp, Optical Soundings and Sounding Rockets, Leibniz Institute of Atmospheric Physics, Schloss-Str. 6, D-18225 Kühlungsborn, Germany. (rapp@iap-kborn.de)